Free-volume structure of fluoropolymer-based radiation-grafted electrolyte membranes investigated by positron annihilation lifetime spectroscopy

2010 J. Phys.: Conf. Ser. 225 012048

(http://iopscience.iop.org/1742-6596/225/1/012048)

Journal of Physics: Conference Series **225** (2010) 012048 doi:10.1088/1742-6596/225/1/012048

Free-volume structure of fluoropolymer-based radiation-grafted electrolyte membranes investigated by positron annihilation lifetime spectroscopy

S Sawada[1], A Kawasuso[2], M Maekawa[2], A. Yabuuchi[2], Y Maekawa[1]

[1]Quantum Beam Science Directorate, Japan Atomic Energy Agency
1233 Watanuki, Takasaki, Gunma 370-1292, Japan
[2] Advanced Research Institute, Japan Atomic Energy Agency
1233 Watanuki, Takasaki, Gunma 370-1292, Japan

E-mail: sawada.shinnichi@jaea.go.jp

Abstract. In the field of polymer-electrolyte-membrane (PEM) fuel cell technology, the structures of free-volume holes in the PEMs are very important because they are correlated to the supplied-gas crossover phenomenon, which sometimes deteriorates the cell performance. In this study, we investigated the size and location of free-volume holes in the crosslinked-polytetrafluoroethylene (cPTFE) based radiation-grafted PEMs by positron annihilation lifetime (PAL) spectroscopy. For comparison, the base cPTFE and polystyrene grafted films were also measured. From the analysis of PAL spectra, it was found that there were free-volume holes with different radius of 0.28-0.30 nm and 0.44-0.45 nm. The smaller holes should be located in both PTFE crystallites and poly(styrene sulfonic acid) grafts, while the larger holes are considered to exist in amorphous PTFE phases.

1. Introduction

Polymer electrolyte membrane (PEM) fuel cells are electrochemical devices to directly transform hydrogen and oxygen into electric power. In a fuel cell, protons dissociated from hydrogen at an anode are transported through a PEM to a cathode, and then react with oxygen to yield water. Recently, there has been increasing interest in PEM fuel cells due to high energy-conversion efficiency and a low environmental load [1-2]. The vital component in the fuel cell is a PEM, which acts as both an electrolyte transporting protons and a separator to prevent mixing of the supplied fuel gases. At present, the most commonly used PEM material is Nafion (DuPont Co.,), consisting of hydrophobic polytetrafluoroethylene (PTFE) backbones with pendent side chains of perfluorinated vinyl ethers terminated by sulfonic acid groups [3]. Although Nafion has excellent properties (proton conductivity, chemical stability, and mechanical strength), it is still too expensive owing to the complicated production process.

During the operation of a PEM fuel cell, supplied hydrogen and oxygen gases permeate through a PEM. This so-called gas crossover phenomenon means the loss of fuel, resulting in deterioration of cell performance [4-9]. Additionally, gas crossover is said to cause a more serious problem. When

oxygen permeates through a PEM from a cathode to an anode, oxygen and proton react to form hydrogen peroxide, which would degrade the PEM [9]. In general, gas diffusion phenomena in a polymer film is believed to be related to the nanometer-sized free-volume holes [10-13]. Consequently, in order to develop the advanced PEM materials with low gas crossover, it is important to obtain a deep insight into the micro-hole structures.

The positron annihilation lifetime (PAL) spectroscopy is capable of directly probing the nanometer-sized free-volume holes. This technique was developed based on the formation of positronium (Ps), the bound state between a positron and an electron. When positrons are injected into materials, there exist three states of positrons with different lifetimes. The shortest-lifetime (~ 0.125 ns) state is *para*-positronium (*p*-Ps), in which the spins are anti-parallel. The middle-lifetime (~ 0.45 ns) state is a free positron without forming a bound state. The longest-lifetime (1-10 ns) state is *ortho*-positronium (*o*-Ps) with parallel spins. The *o*-Ps lifetime has a strong correlation with the size of the free-volume holes: that is, as the holes become smaller, the *o*-Ps lifetime decreases. Therefore, the information of free-volume structures in materials can be obtained by PAL spectra.

As a low-cost process of PEM synthesis, a radiation-induced grafting method has been widely focused [14,15]. This method consists of the following three steps: irradiation to fluoropolymer base films; grafting of styrene from generated radicals; and sulfonation of grafted films. The resultant PEM possesses the fluoropolymer back bones and poly(styrene sulfonic acid) (PSSA) graft chains. In this method, one can widely control the degree of grafting (DOG) by various grafting conditions.

In this study, we investigated the micro-hole structures in the radiation-grafted PEMs by using PAL spectroscopy measurement. The target materials are the PEMs based on crosslinked-polytetrafluoroethylene (cPTFE) films developed by our research group [16]. Up to now, there have been several reports on PAL measurement of Nafion [17,18]. On the contrary, as far as the authors know, little is known about free-volume holes in the radiation-grafted PEMs. In this study, we clarify the size and location of microvoids in the cPTFE-based grafted PEMs.

2. Experimental

2.1. Synthesis of PEMs

The PEMs were synthesized as already reported [16]. We used, as a base material, a 42-μm thick film of PTFE crosslinked with an electron beam at 100 kGy. The film was pre-irradiated with 15-kGy γ-ray in an Ar atmosphere at room temperature and then immersed in a styrene monomer at 60 °C for 2-18 h. After the grafting reaction, the film was immersed in toluene to extract any excess styrene. The grafted film was then dried under vacuum at 50 °C to a constant weight. The degree of grafting (DOG) was estimated by:

$$\mathrm{DOG} = \frac{W_G - W_O}{W_O} \times 100 \qquad (1)$$

where W_G and W_O denote the weights of the grafted and base films, respectively.

For sulfonation, the grafted film was immersed in 0.2 M chrolosulfonic acid / 1,2-dichloroethane mixture at 50 °C for 6 h. Finally, the obtained PEM was rinsed with pure water and then dried in a vacuum oven.

2.2. PAL measurement

PAL measurements were carried out using conventional “fast-fast” coincidence system with a time resolution of 225 ps. A ^{22}Na positron source was prepared by depositing and drying aqueous solution of ^{22}NaCl on a Kapton thin film. This substrate (1 cm × 1 cm) was covered with another Kapton film with the same size. The edges were glued to seal activity inside.

The PEMs were measured in the dried and fully-hydrated states at 300 K. A stack of about 10 PEM samples was set on each side of the positron-source Kapton films to ensure positron annihilation only in the samples. All the PAL measurements were conducted at the room temperature. The

obtained PAL spectra with about 10^6 counts were analyzed by PATFIT program. For comparison, the virgin cPTFE and styrene-grafted films were also measured in a similar way.

3. Results and discussion

3.1. Styrene-grafted films with different DOGs

The PAL spectra for all the samples were deconvoluted into four components with lifetimes, τ_i, and intensities, I_i. In three-component analysis, the accuracy of spectra fitting was not good. The detected four components were numbered 1, 2, 3, and 4 from the shortest to the longest lifetime. Components 1 and 2 are surely *p*-Ps and free-positron, respectively. Components 3 and 4 are attributed to two types of *o*-Ps in different regions.

Figure 1 and 2 shows the lifetimes (τ_3 and τ_4) and relative intensities (I_3 and I_4) of the two types of *o*-Ps in the styrene-grafted films. For the base cPTFE film (see the plots at DOG = 0), τ_3 and τ_4 were 2.3 and 4.5 ns, respectively. In order to considerate the location of *o*-Ps, we should take into account very high crystallinity of PTFE, i.e., PTFE matrices consist of both crystalline and amorphous phases. In the former, the polymer chains are regularly and densely packed with small intermolecular free-volume voids. On the other hand, in the latter, the polymer chain arrangement is random, thereby forming larger-sized free-volume spaces between chains. Accordingly, component 3 and 4 are likely *o*-Ps in the PTFE crystalline and amorphous regions, respectively. Also, in the previous report concerning PAL measurement on PTFE films (non crosslinked) [19], the shorter- and longer-lived *o*-Ps were assumed to be in crystalline and amorphous regions, respectively.

As the DOG increased, both τ_4 and I_4 exhibited declining trends, indicating the structural change in the amorphous regions. This result can be explained by considering the radiation grafting process as follows. The grafting reaction should initiate from polymer radicals generated by pre-irradiation, located in the crystalline / amorphous interfacial layers. The polystyrene graft chains would be elongated into amorphous regions, leading to a decrease of both the size and number of free-volume holes (low τ_4 and low I_4). The similar phenomenon was observed in the PAL study for the other polystyrene-grafted film based on poly(tetrafluoro-ethylene-*co*-hexafluoropropylene) [20].

On the other hand, I_3 was raised with a DOG (see Fig. 2). From this result, one may possibly suspect that PTFE crystallites became larger in the highly-grafted film. However, this is never true. In

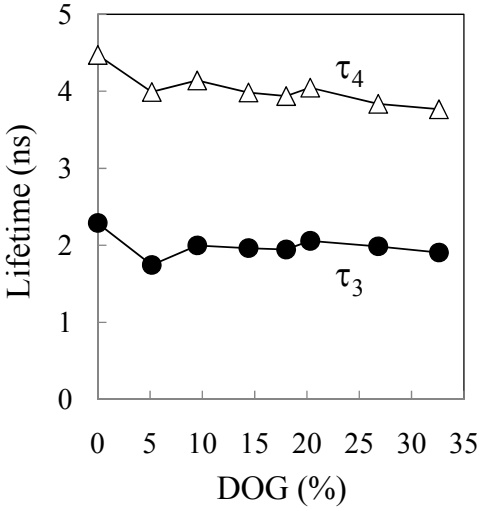

Figure 1. Lifetimes of (●) τ_3 and (△) τ_4 in the styrene-grafted cPTFE films. The plots at DOG = 0 are the results for the base cPTFE film.

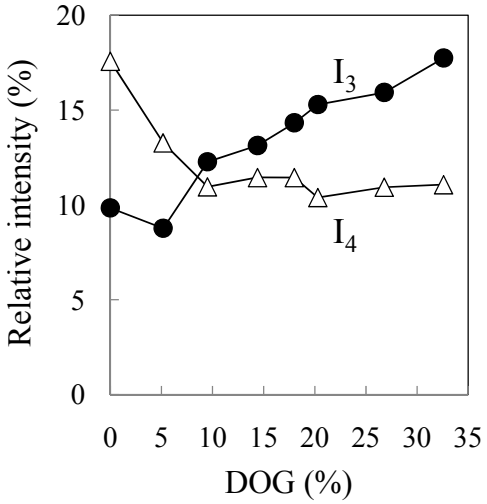

Figure 2. Relative intensity of (●) I_3 and (△) I_4 in the styrene-grafted cPTFE films. The plots at DOG = 0 are the results for the base cPTFE film.

general, the graft chain elongation leads to a disruption of polymer crystallites. Then, the relationship between I_3 and a DOG was rationalized as follows. According to the previous report [21], the *o*-Ps lifetime in polystyrene powders was about 1.9 ns, which is similar to τ_3 in the PTFE crystallites. Consequently, component 3 for styrene-grafted PTFE films is considered to be *o*-Ps not only in PTFE crystallites but also in grafted polystyrene phases. This is the reason why I_3 increased with a DOG.

3.2. Styrene-grafted films and PEMs

Figure 3 and 4 show the lifetimes and relative intensities of components 2, 3, and 4 for the grafted films and PEMs (DOG is 14% and 27%). The most significant change was observed in I_2 as shown in Fig. 3 (B) and Fig. 4 (B). Compared to grafted films, I_2 of the dried PEMs remarkably increased up to about 60%, while both I_3 and I_4 decreased. Similar observation was already reported in a previous study [22], in which the PAL measurements were performed on poly(ether ether ketone) (PEEK) films before and after sulfonation. The yield of *o*-Ps was found to be very low in sulfonated PEEK (sPEEK) compared with that in non-sulfonated one. Such a phenomenon is called inhibition of Ps formation, and is presumed to be caused by the following mechanism. Since the sulfonic acid group is an electron withdrawing component, the aromatic ring substituted by it becomes electron deficient and electron accepting. Some of the spur electrons likely tend to be captured by these electron acceptors (sulfonated aromatic rings), and hence cannot recombine with positrons to form Ps. Namely, there were not sufficient available electrons to react, which would suppress the Ps formation. In our cPTFE-based PEMs possessing the poly(styrene sulfonic acid) (PSSA) graft chains, the above-mentioned electron-scavenging process probably occurred, resulting in a decrease of both I_3 and I_4.

The τ_4 in the PEMs was higher than that in the styrene-grafted films at both DOGs. This τ_4 increase was related to the structural change in the PTFE amorphous phases, and can be accounted for as follows. In the grafted films (before sulfonation), the polystyrene graft chains should be somewhat entangled with amorphous PTFE chains. On the contrary, in the PEMs obtained by sulfonation, the repulsive interactions likely acted between the PSSA graft and PTFE chains because their chemical properties were quite different. In other words, they are completely immiscible each other (The PSSA is hydrophilic, while the PTFE is hydrophobic.). Then, the PSSA grafts may be phase-separated from the PTFE chains. Consequently, the PTFE amorphous phases, from which the PSSA chains were excluded out, should be more vacant and had more free-volume spaces (higher τ_4).

3.3. Dried and fully-hydrated PEMs

As already mentioned, the *o*-Ps lifetime has a strong correlation with the size of free-volume holes. The annihilation of *o*-Ps in the spherical holes is described by simple quantum mechanical model with infinite height potential. The semi-empirical relationship between the *o*-Ps lifetime, τ (ns), and radius of free-volume holes, R (nm), was expressed by the following Tao-Eldrup equation:

$$\tau = \frac{1}{2}\left[1 - \frac{R}{R+\Delta R} + \frac{1}{2\pi}\sin\left(\frac{2\pi R}{R+\Delta R}\right)\right]^{-1}, \qquad (2)$$

where ΔR denotes a fitted empirical electron-layer thickness (=0.166 nm). The hole volume, V (nm^3), is calculated by:

$$V = \frac{4}{3}\pi R^3. \qquad (3)$$

Table 1 and 2 show the R values calculated by equation (2), as well as the measured *o*-Ps lifetimes. The V calculated by substituting the R into equation (3) is also shown in Table 1 and 2. The V in the dried PEMs with different DOGs were almost the same each other. The V corresponding to τ_3 and τ_4 were estimated to be 0.11 nm^3 and 0.36-0.38 nm^3, respectively. The smaller holes should be in both PTFE crystallites and PSSA grafts, while the larger holes are likely in the amorphous PTFE phases. According to the previous report [23], the self-diffusion coefficient, D, of various gases

including oxygen was found to be proportional to the inverse of V. From this relationship of D versus 1/V, the D of oxygen in the cPTFE PEMs was roughly evaluated to be on the order of 10^{-7} cm^2/s in the smaller holes and 10^{-4} cm^2/s in larger holes.

A final topic in this paper is the effect of hydration level on the micro-hole structures. Notice that τ_3 was a little smaller in the fully-hydrated states than in dried ones (see Fig. 3(A) and 4(A)). The calculated V values in the PEMs with DOGs of 14 and 27% were 0.10 and 0.092 nm^3, respectively (see Table 1 and 2). Although the above τ_3 decrease is within an experimental error, it implies the meaningful structural change in PEMs. When the PEMs were hydrated, PSSA graft chains should alter their conformations because absorbed water gathered around the sulfonic acid groups, which possibly made micro holes smaller. Sodaye et al. also reported the similar findings in Nafion [18]: As the water content increased, the size of free-volume holes decreased. In the near future, we are planning to

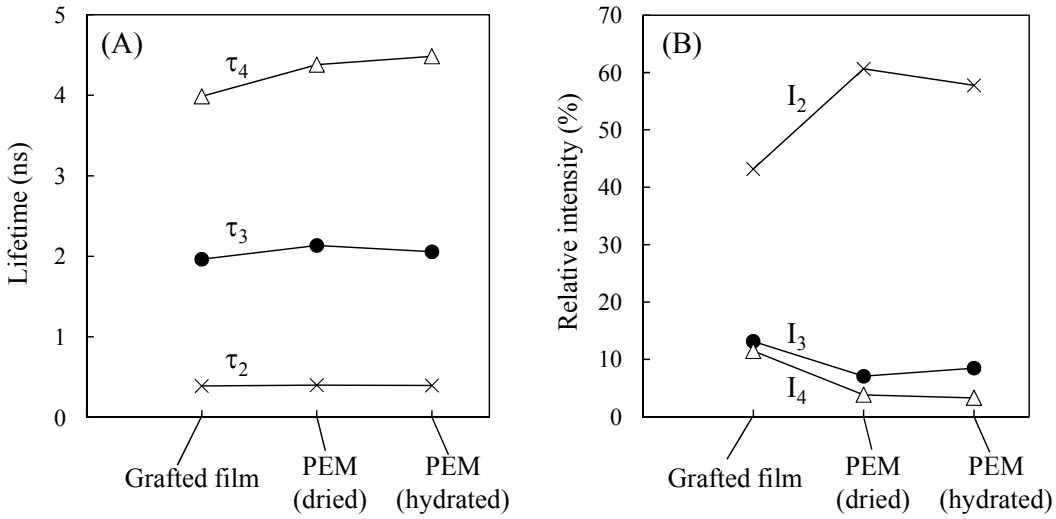

Figure 3 (A) Lifetimes and (B) relative intensities of component 1, 2, and 3 in the grafted film and PEM with a DOG of 14%.

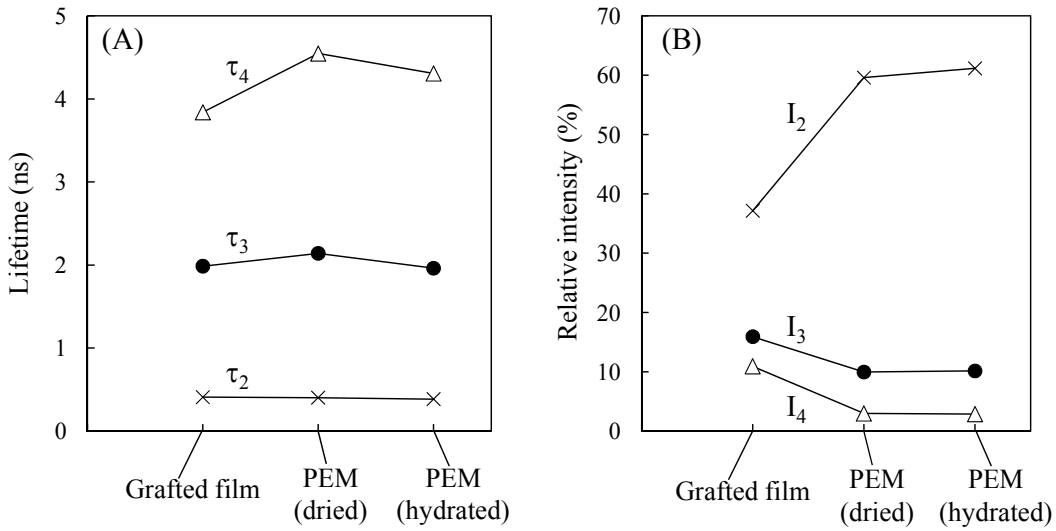

Figure 4 (A) Lifetimes and (B) relative intensities of component 1, 2, and 3 in the grafted film and PEM with a DOG of 27%.

perform the PAL measurements on PEMs under the controlled temperature and relative humidity. In addition, the permeability of hydrogen and oxygen through PEMs will be measured.

Table 1 Lifetimes of *o*-Ps, R, and V in the PEMs with a DOG of 14%

	Component 3		Component 4	
	dried	hydrated	dried	hydrated
τ_3 (ns)	2.1	2.1	4.4	4.5
R (nm)	0.30	0.29	0.44	0.45
V (nm^3)	0.11	0.10	0.36	0.38

Table 2 Lifetimes of *o*-Ps, R, and V in the PEMs with a DOG of 27%

	Component 3		Component 4	
	dried	hydrated	dried	hydrated
τ_3 (ns)	2.1	2.0	4.5	4.3
R (nm)	0.30	0.28	0.45	0.44
V (nm^3)	0.11	0.092	0.38	0.36

References

[1] Smitha B, Sridhar S and Khan A A 2005 J. Membr. Sci. **259** 10
[2] Dobrovol' skii Y A, Volkov E V, Pisareva A V, Fedotov Y A, Likhachev D Y and Rusanov A L 2007 Russ. J. Gen. Chem. **77** 766
[3] Mauritz K A and Moore R B 2004 Chem. Rev. **104** 4535
[4] Büchi F N, Gupta B, Haas O and Scherer G G 1995 J. Electrochem. Soc. **142** 3044
[5] Büchi F N, Gupta B, Haas O and Scherer G G 1995 Electrochim. Acta **40** 345
[6] Wang H and Capuano G A 1998 J. Electrochem. Soc. **145** 780
[7] Vie P, Paronen M, Strømgård M, Rauhala E and Sundholm F 2002 J. Membr. Sci. **204** 295
[8] Schmidt T J, Simbeck K and Scherer G G 2005 J. Electrochem. Soc. **152** A93
[9] Inaba M, Kinumoto T, Kiriake M, Umebayashi R, Tasaka A and Ogumi Z 2006 Electrochim. Acta **51** 5746
[10] Haraya K and Hwang S T 1992 J. Membr. Sci. **71** 13
[11] Tanaka K, Katsube M, Okamoto K, Kita H, Sueoka O and Ito Y 1992 Bull. Chem. Soc. Jpn. **65** 1891
[12] Budd P M, Mckeown N B and Fritsch D 2005 J. Mater. Chem. **15** 1977
[13] Fu Y J, Hu C C, Lee K R, Tsai H A, Ruaan R C and Lai J Y 2007 Euro. Polym. J. **43** 959
[14] Nasef M M and Hegazy E S A 2004 Prog. Polym. Sci. **29** 499
[15] Gubler L, Gürsel S A and Scherer G G 2005 Fuel Cells **5** 317
[16] Yamaki T, Kobayashi K, Asano M, Kubota H and Yoshida M 2004 Polymer **45** 6569
[17] Sodaye H S, Pujari P K, Goswami A and Manohar S B 1997 J. Polym. Sci. B: Polym. Phys. **35** 771
[18] Sodaye H S, Pujari P K, Goswami A and Manohar S B 1998 J. Polym. Sci. B: Polym. Phys. **36** 983
[19] Mohamed H F M, Abdel-Hady E E and Mohamed S S 2007 Radiat. Phys. Chem. **76** 160
[20] Sudarshan K, Rath S K, Patri M, Sachdeva A and Pujari P K 2007 Polymer **48** 6434
[21] Honda Y, Shimada T, Tashiro M, Kimura N, Yoshida Y, Isoyama G and Tagawa S 2007 Radiat. Phys. Chem. **76** 169
[22] Kobayashi Y, Mohamed H F M and Ohira A 2009 J. Phys. Chem. B **113** 5698
[23] Kobayashi Y, Haraya K, Hattori S and Sasuga T 1994 Polymer **35** 925